AJNR

Identification of Vortex Cores in Cerebral Aneurysms on 4D Flow MRI

K. Futami, T. Uno, K. Misaki, S. Tamai, I. Nambu, N. Uchiyama and M. Nakada

Identification of Vortex Cores in Cerebral Aneurysms on 4D Flow MRI

K. Futami, T. Uno, K. Misaki, S. Tamai, I. Nambu, N. Uchiyama, and M. Nakada

ABSTRACT

BACKGROUND AND PURPOSE: The complexity and instability of the vortex flow in aneurysms are factors related to the rupture risk of unruptured cerebral aneurysms. We identified aneurysm vortex cores on 4D flow MR imaging and examined the relationship of these factors with the characteristics of cerebral aneurysms.

MATERIALS AND METHODS: We subjected 40 aneurysms (37 unruptured, 3 ruptured) to 4D flow MR imaging. We visualized streamlines with velocities below the threshold—that is, a percentage value of the aneurysm maximum inflow velocity—and progressively decreased the threshold to identify vortex cores as thin, streamline bundles with minimum velocities. Complexity and stability were compared in aneurysms with a smooth surface and those with blebs or daughter sacs.

RESULTS: The threshold for visualizing vortex cores ranged from 3% to 13% of the maximum inflow velocity. Vortex cores could be visualized in 38 aneurysms; in 2, they were not visualized through the cardiac cycle. A simple flow pattern (single vortex core) was identified in 27 aneurysms; the other 13 exhibited a complex flow pattern. The cores were stable in 32 and unstable in 8 aneurysms. Significantly more aneurysms with-than-without blebs or daughter sacs had a complex flow pattern ($P = .006$). Of the 3 ruptured aneurysms, 1 aneurysm had an unstable vortex core; in the other 2, the vortex core was not visualized.

CONCLUSIONS: The identification of vortex cores on 4D flow MR imaging may help to stratify the rupture risk of unruptured cerebral aneurysms.

ABBREVIATION: CFD = computational fluid dynamics

Rupture-risk stratification is crucial to decide appropriate treatments for unruptured cerebral aneurysms to avoid profound complications elicited by invasive treatments. The complexity and instability of the intra-aneurysmal vortical flow have been correlated with the rupture risk of unruptured cerebral aneurysms.[1-4] The vortex core line, a skeleton of the vortical flow and defined on the basis of various mathematic definitions,[5,6] facilitates the qualitative and quantitative evaluation of the complexity and instability of the intra-aneurysmal flow of aneurysm models using computational fluid dynamic (CFD) simulations.[1-4,7,8] However, CFD analysis is based on assumptions and approximations regarding blood properties, vessel wall compliance, and flow conditions,[1-4] and the location of the vortex core line depends on mathematic

definitions.[8] Although 4D flow MR imaging, based on time-resolved 3D cine phase-contrast MR imaging techniques, has been used to evaluate the hemodynamics in human cerebral aneurysms,[9-12] the visualization of aneurysm vortex cores with this imaging technique has not been reported. Identification of vortex cores on 4D flow MR imaging may be an alternative to CFD analysis of aneurysm models and may lead to new insights into the role of vortex cores in aneurysm behavior.

In this study, we identified vortex cores by showing streamlines with minimum flow velocities in cerebral aneurysms and examined the relationship between the complexity and stability of the vortex core and the characteristics of cerebral aneurysms.

MATERIALS AND METHODS

The institutional review board of Hokuriku Cetral Hospital approved this study; prior informed consent was obtained from all patients.
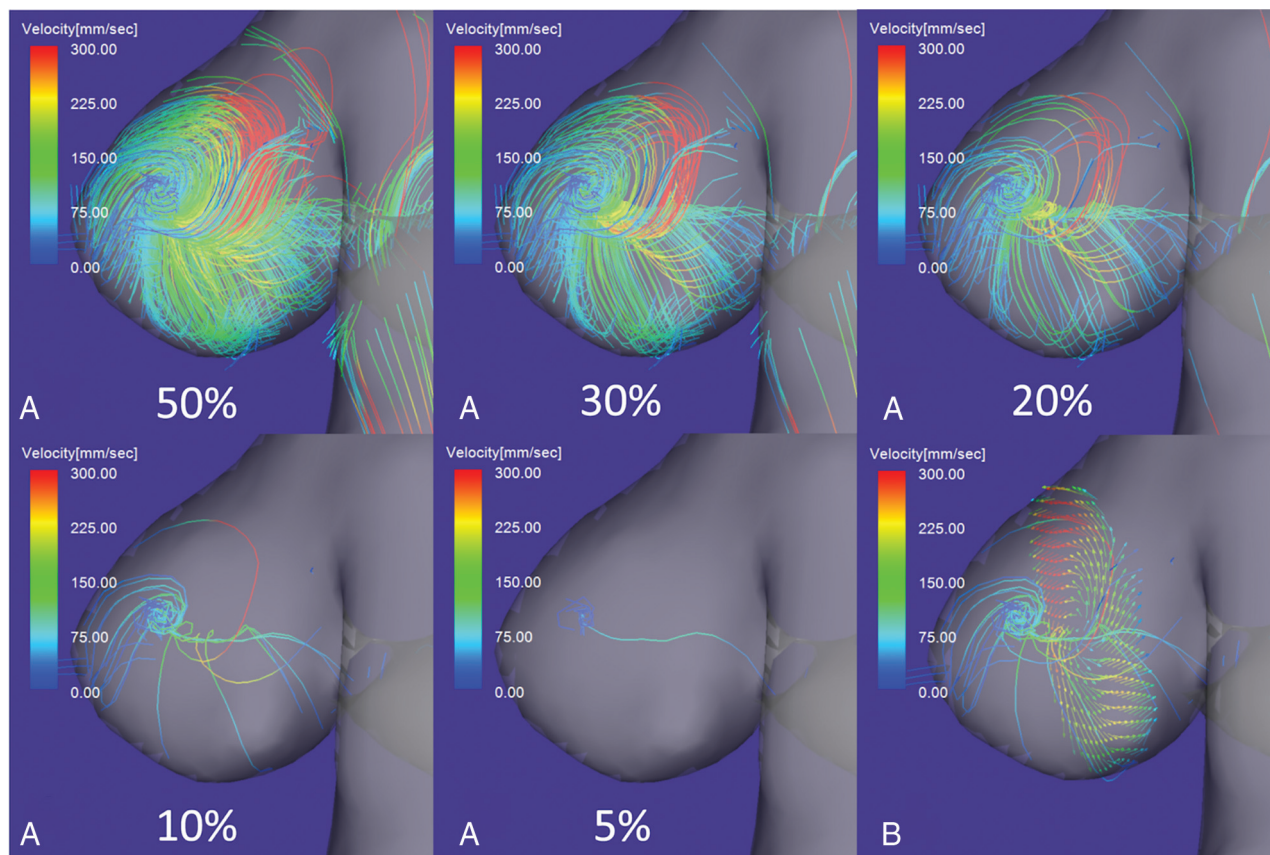
This study included 35 patients (13 men, 22 women; mean age, 68.2 ± 10.8 years; range, 41–89 years) with 40 aneurysms (37 unruptured, 3 ruptured). They were located on the cavernous

FIG 1. 4D flow MR images of flow streamlines with velocities below the threshold determined by the percentage value of the maximum inflow velocity. *A*, When the threshold was decreased from 30% to 10% of the maximum inflow velocity, a single vortex core was visualized as a thin, streamline bundle. At a threshold of 5%, the vortex core was a single line. *B*, A thin, streamline bundle passed through the center of vortical flow vectors on a cutting plane of the aneurysm dome.

segment ($n = 1$), the paraclinoid segment ($n = 10$), and the communicating segment ($n = 5$) of the ICA; the ICA bifurcation ($n = 1$); the MCA bifurcation ($n = 12$); the A1 segment of the anterior cerebral artery ($n = 1$); the anterior communicating artery ($n = 5$); and the tip of the basilar artery ($n = 5$). The maximum diameter and neck size were 6.5 ± 2.8 mm (range, 4.0–15.0 mm) and 5.0 ± 2.1 mm (range, 2.5–11.3 mm), respectively. Their sizes exceeded the spatial resolution of 4D flow MR imaging.[11,12]

MRI
We used a 1.5T MR imaging scanner (Magnetom Avanto; Siemens, Erlangen, Germany) with a slew rate of 125 T/m/s and an 8-channel head array coil. Contrast-enhanced MRA was performed after the injection of 0.2 mL/kg of gadodiamide delivered via an 18- or 20-ga cannula at a rate of 1 mL/s into the antecubital vein. The scanning parameters were the following: TR/TE/NEX, 4.65/1.74 ms/average 1; flip angle, 20°; band width, 330 Hz/pixel; FOV, 180 × 180 mm; section thickness, 0.7 mm; 1 slab; 60 sections/slab; voxel size, 0.6 × 0.6 × 0.7 mm; transaxial direction.

The parameters for phase-contrast MR imaging were the following: TR/TE/NEX, 33.05/5.63 ms/average 1; flip angle, 22°; band width, 434 Hz/pixel; FOV, 200 × 200 mm; section thickness, 0.8 mm; 1 slab; 24–26 sections/slab; z-coverage, 19.2 mm; matrix, 192 × 192; no interpolation processing; voxel size, 1.04 × 1.04 × 0.8 mm; velocity encoding, 40–60 cm/s; parallel imaging

with reduction factor, 2; imaging time, 20–30 minutes depending on the patient's heart rate; transaxial direction; retrospective gating with an electrocardiogram; temporal resolution, 0.0333 seconds.

Commercially available software (Flova II, Version 2.10.7.0; R'Tech, Hamamatsu, Japan) was used to visualize flow vectors and streamlines on the basis of 3D blood flow information obtained by 4D flow MR imaging. The vascular wall was reconstructed with region-growing[13] and marching cubes[14] methods applied to datasets obtained by contrast-enhanced MRA. The 3D datasets acquired by phase-contrast MR imaging were converted to voxel datasets at a spatial resolution of 0.5 × 0.5 × 0.5 mm using a vender-provided function.

By means of the Runge-Kutta method,[15] streamlines were constructed by integrating flow vectors in the whole intra-aneurysmal region and in close parent arteries. They were visualized at a density of 16 lines/mm². Because streamlines constructed with forward integration tended to conceal flow structures inside the vortices, we used backward-integration exclusively to visualize the vortex cores.

Data Analysis
By means of a Flova II function, an arbitrary percentage value of the maximum inflow velocity in the aneurysm orifice can be selected as the visualization threshold of flow streamlines in the aneurysm. Byrne et al[3] reported that a vortex core line can be
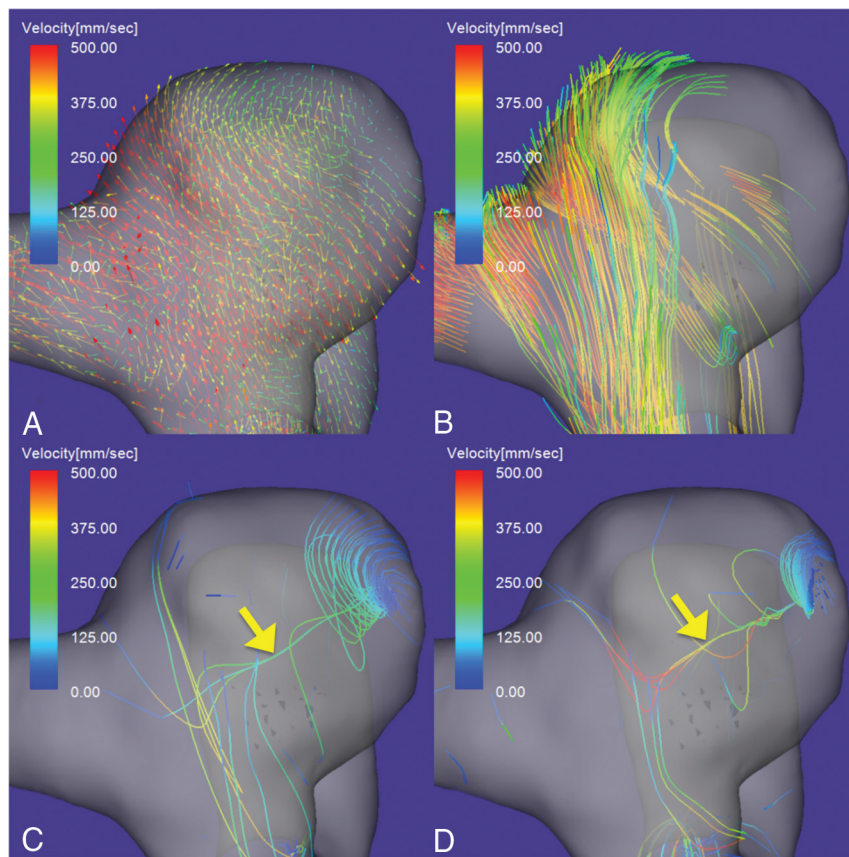
FIG 2. 4D flow MR images of an unruptured aneurysm on the paraclinoid segment of the right ICA. *A,* Flow vector map. *B,* The inflow jet is visualized as a layer of streamlines with high velocities. A single stable vortex core (*yellow arrow*) is visualized in the diastolic (*C*) and systolic (*D*) phases of the cardiac cycle. The vortex core is visualized as a bundle of streamlines with velocities below 7% (*C*) and 10% (*D*) of the maximum inflow velocity. The aneurysm flow pattern is simple and stable.

Table: Complexity and stability of vortex cores in cerebral aneurysms[a]

Aneurysm	Complexity Simple/Complex	Stability Stable/Unstable
Smooth wall (*n* = 25)	21 (84.0%)/4 (16.0%)	22 (88.0%)/3 (12.0%)
Irregular wall (*n* = 15)	6 (40.0%)/9 (60.0%)	10 (66.7%)/5 (33.3%)
P value	.006 (S)	.126 (NS)

Note:—NS indicates not significant; S, significant on the Fisher exact test.
[a] Simple and complex flow patterns were defined as exhibiting a single vortex core or multiple or nonvisualized vortex cores through the cardiac cycle, respectively. Stable and unstable flow patterns were defined as exhibiting persistent vortex cores or moving or nonvisualized vortex cores, respectively. The designation of "irregular wall" was recorded when the wall had protruding blebs or daughter sacs. Differences of $P < .05$ were considered significant.

constructed by connecting the points along the faces containing the zeros of the reduced velocity in cerebral aneurysms. We visualized the vortex cores as thin, streamline bundles composed of streamlines with velocities below the threshold, which was determined by progressively decreasing the percentage value of the maximum inflow velocity in each aneurysm. The maximum inflow velocity was measured on the aneurysm orifice plane using 4D flow MR imaging as the maximum value during the cardiac cycle.

We defined simple flow patterns as those with a single vortex core and complex flow patterns as those with multiple or

nonvisualized vortex cores through the cardiac cycle. Stable flow patterns were defined as those with persistent vortex cores; unstable flow patterns, as those with moving or nonvisualized vortex cores. Because aneurysms with no visualized vortex cores through the cardiac cycle had multiple small vortices beneath the aneurysm surface and irregular streamlines, we attributed this observation to the presence of an extremely complex and unstable intra-aneurysmal flow and recorded them as exhibiting a complex and unstable flow pattern.

We compared the complexity and stability of aneurysms with a smooth surface and those with an irregular wall characterized by blebs or daughter sacs. Three observers (K.F., T.U., and K.M.) independently recorded the number and location of vortex cores. Disagreements were settled by consensus.

For statistical analysis we used the Fisher exact test for categoric variables. Differences of *P* value < .05 were considered significant.

RESULTS

Figure 1*A* shows aneurysm flow streamlines with velocities below the threshold determined by progressively decreased percentage values of the maximum inflow velocity of the aneurysm. A single vortex core was observed as a thin, streamline bundle when the threshold was decreased from 30% to 10% of the maximum inflow velocity; at the 5% threshold, the vortex core was a single line. A thin, streamline bundle passed through the center of vortical flow vectors on a cutting plane of the aneurysm dome (Fig 1*B*). On en face views of the inflow jet of aneurysms, most vortex cores were orthogonal to the inflow jet (Fig 2*B*). Because the threshold value appropriate for visualizing the vortex cores of individual aneurysms depended on the systolic or diastolic phase of the cardiac cycle and on the vortex core per se, we progressively decreased the threshold by 1% for each aneurysm. Consequently, the threshold for assessing the vortex cores ranged from 3% to 13% of the maximum inflow velocity.

Vortex cores could be identified in 38 of the 40 aneurysms; in the other 2, they were not visualized through the cardiac cycle. As shown in the Table, a simple flow pattern (single vortex core) was visualized in 27 aneurysms; the other 13 exhibited a complex flow pattern. The vortex core was stable in 32 aneurysms and unstable in the other 8. There were 15 aneurysms with an irregular wall: Six manifested a simple pattern, and 9, a complex flow pattern. The vortex core was stable in 10 and unstable in 5 of these aneurysms (*P* = .126). The incidence of a complex flow pattern was significantly higher in aneurysms with an irregular wall
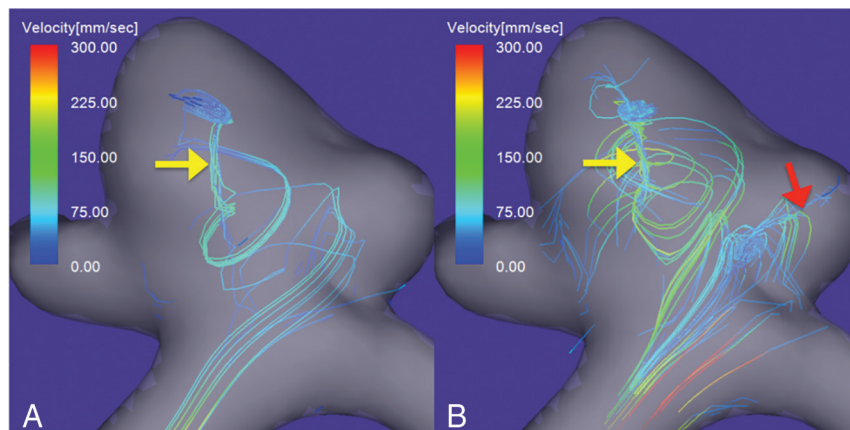
FIG 3. An unruptured right MCA bifurcation aneurysm with a daughter sac. Vortex cores in the diastolic (*A*) and systolic (*B*) phases of the cardiac cycle. A single vortex core is visualized in the diastolic phase (*A*, *yellow arrow*), and another, in the systolic phase (*B*, *red arrow*). The vortex cores are visualized as bundles of streamlines with velocities below 4% and 7% of the maximum inflow velocity in the diastolic and systolic phases, respectively. The flow pattern was recorded as complex.
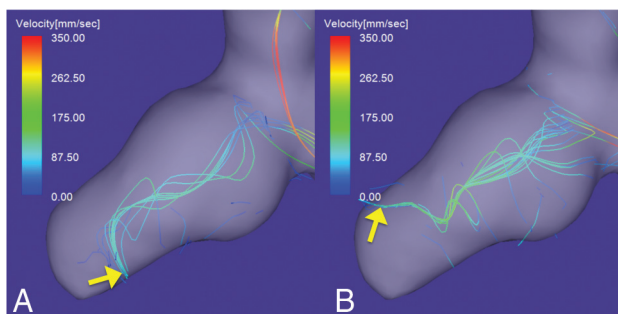
FIG 4. A ruptured right ICA aneurysm with a daughter sac. The vortex core in the diastolic (*A*) and systolic (*B*) phases of the cardiac cycle. The vortex core in both phases is visualized as a bundle of streamlines with velocities below 4% of the maximum inflow velocity. The direction of the tip of the vortex core markedly changes during the cardiac cycle (*yellow arrows*). The flow pattern was recorded as unstable.

($P = .006$). Of the 3 ruptured aneurysms, 1 aneurysm exhibited an unstable vortex core; in the other 2, multiple small vortices beneath the aneurysm surface and irregular streamlines were visualized, while no vortex cores were visualized through the cardiac cycle.

Case Presentation

Case 1. A 61-year-old woman presented with an unruptured aneurysm on the paraclinoid segment of the right ICA (Fig 2). The maximum aneurysm diameter and neck size were 7.3 and 5.5 mm, respectively. The maximum inflow velocity was 710 mm/s. A vortex core was visualized as a bundle of streamlines with velocities below the 7% value and below the 10% value of the maximum inflow velocity in the diastolic and systolic phases, respectively (Fig 2C, -D). The vortex core was single and stable through the cardiac cycle. The vortex core was orthogonal to the inflow jet in the aneurysm (Fig 2B). This aneurysm flow pattern was recorded as simple and stable.

Case 2. A 52-year-old man presented with an unruptured right MCA bifurcation aneurysm with a daughter sac (Fig 3). The maximum aneurysm diameter and neck size were 6.5 and 4.1 mm, respectively. The maximum inflow velocity was 580 mm/s. During the diastolic phase of the cardiac cycle, only 1 vortex core could be visualized (yellow arrow in Fig 3A). However, during the systolic phase, another vortex core was observed; it was directed toward the tip of the daughter sac (red arrow in Fig 3B). These vortex cores were visualized as bundles of streamlines with velocities below the 4% and 7% values of the maximum inflow velocity in the diastolic and systolic phases, respectively. The flow pattern was recorded as complex.

Case 3. A 53-year-old man presented with a ruptured right ICA aneurysm with a daughter sac on the tip of the aneurysm (Fig 4). The maximum aneurysm diameter and neck size were 8.7 and 3.5 mm, respectively. The maximum inflow velocity was 620 mm/s. In the diastolic (Fig 4A) and systolic phases (Fig 4B), a vortex core was visualized as a bundle of streamlines with velocities below 4% of the maximum inflow velocity. The vortex core was directed from the aneurysm neck to the daughter sac. The direction of the tip of the vortex core was markedly different during the diastolic and systolic phases (yellow arrows in Fig 4A, -B). The flow pattern was recorded as unstable.

Case 4. A 73-year-old man presented with a large ruptured aneurysm on the tip of the basilar artery (Fig 5). The maximum aneurysm diameter and neck size were 15.0 and 11.3 mm, respectively. The maximum inflow velocity was 820 mm/s. 4D flow MR imaging acquired through the cardiac cycle revealed multiple small vortices beneath the aneurysm surface and irregular streamlines in the aneurysm (Fig 5B, -C). No vortex cores were visualized.

DISCUSSION

We first report that vortex cores in cerebral aneurysms can be identified and evaluated on 4D flow MR imaging, and we document that the incidence of complex flow patterns was significantly higher in aneurysms with blebs or daughter sacs.

A complex and unstable flow pattern is a rupture risk for cerebral aneurysms.[1-4] Xiang et al,[2] who performed CFD analysis in 38 ruptured and 81 unruptured aneurysms, found that rupture was strongly correlated with a complex flow pattern characterized by multiple vortices. Byrne et al[3] evaluated the hemodynamics of 210 aneurysms, including 83 ruptured aneurysms; their CFD analysis showed that ruptured aneurysms manifested a more complex and more unstable flow pattern than unruptured aneurysms. However, Cornelissen et al[16] reported that morphologic changes of aneurysms on rupture might affect the results of hemodynamic analysis of ruptured aneurysms. Risk factors
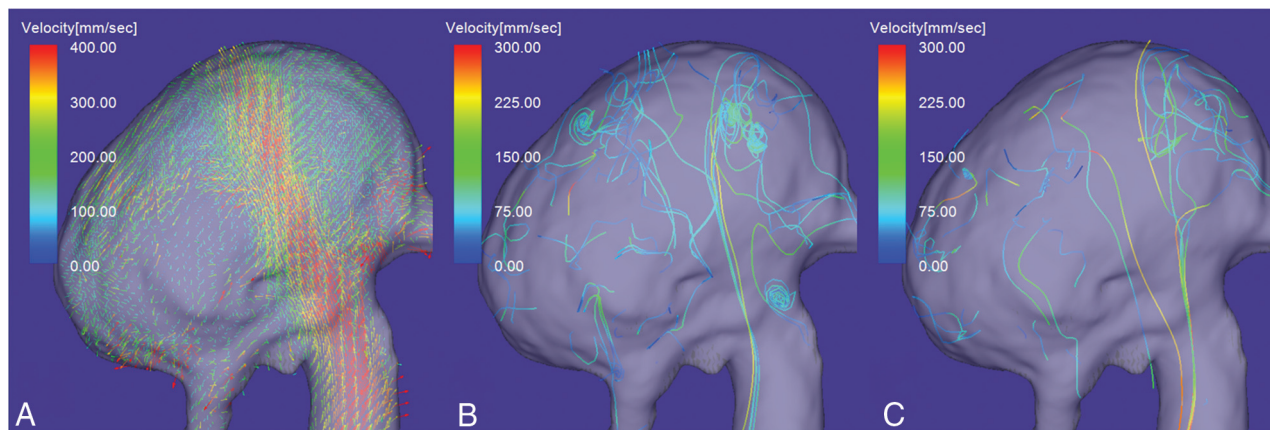
FIG 5. A large ruptured aneurysm on the tip of the basilar artery. *A*, Flow vector map. Streamlines with velocities below 7% of the maximum inflow velocity in the diastolic (*B*) and systolic (*C*) phases. Although multiple small vortices beneath the aneurysm surface and irregular streamlines are visualized, no vortex cores are visualized through the cardiac cycle.

obtained by comparing the hemodynamics of ruptured and unruptured cerebral aneurysms should be interpreted with caution. According to Cebral et al,[17] the complexity and instability of the intra-aneurysmal flow were related to the aneurysm wall property. Therefore, the complexity and instability of the intra-aneurysmal flow should be considered in the evaluation of the rupture risk of unruptured cerebral aneurysms. Although the vortex core line visualized by CFD analysis facilitates the evaluation of the complexity and instability of vortical flows, aneurysm vortex cores have not been identified on 4D flow MR imaging.

Although vortex cores have been extracted on the basis of a variety of mathematic algorithms,[5,6] there is no formal definition.[8] The most widely used algorithm is based on reduced velocity[3] or the velocity gradient tensor, eg, the Q-Criterion or the λ_2-Criterion method.[7,18] Köhler et al[18] compared the vortical structures semiautomatically extracted using different local vortex criteria on 4D flow MR imaging of the aorta and pulmonary artery. They found that the λ_2-Criterion method was most suitable for the extraction of vortices. However, a reliable method to accurately extract the vortex cores of cerebral aneurysms remains to be established. Although Marquering et al[19] and Feliciani et al[20] quantified vortical structures using scale-space techniques on the basis of 4D flow MR imaging of an aneurysm phantom, they did not apply their method to detect and quantify the vortex cores of human cerebral aneurysms. For the extraction of vortex cores, Byrne et al[3] constructed a vortex core line using an algorithm that connects the points along faces containing the zero value of the reduced velocity of intra-aneurysmal vortices. Because Flova II does not feature a mathematic algorithm to extract the vortex cores, we attempted to visualize them by demonstrating the streamlines with minimum velocities. By progressively decreasing the threshold (ie, the percentage value of the maximum inflow velocity), we were able to visualize vortex cores at a range from 3% to 13% of the maximum inflow velocity. Our method is simple and allows visual evaluation of the characteristics of vortex cores in aneurysms.

Blebs or daughter sacs are a risk factor for aneurysm rupture.[21-23] In a prospective study, UCAS Japan investigators[21] followed up 6697 unruptured aneurysms conservatively. They documented that 18.9% featured daughter sacs and that their presence was a risk factor for rupture. Murayama et al[22] performed a prospective 10-year cohort study with a mean follow-up duration of 7388 follow-up years; they also found that daughter sacs were a significant independent predictor of rupture. Additionally, Tsukahara et al[23] reported that the rupture rate during the first year of their observation of all unruptured aneurysms was 3.42%; it was 28.3% for aneurysms with blebs. We found that aneurysms with blebs or daughter sacs had a complex flow pattern at a significantly higher rate than the other aneurysms (P = .006). Of our 3 ruptured aneurysms, 1 aneurysm had an unstable vortex core. In the other 2, we noted multiple small vortices and irregular streamlines that were attributable to an extremely complex and unstable flow; no vortex cores were identified. Corresponding to earlier reports,[1-4] our observations suggest that a complex and unstable intra-aneurysm vortical flow raises the risk for rupture. Moreover, the nonvisualization of vortex cores on 4D flow MR imaging may be related to aneurysm rupture. Therefore, evaluation of vortex cores on 4D flow MR imaging may be useful for the rupture-risk stratification of unruptured cerebral aneurysms.

Our study has some limitations. Flova II is not available for the quantitative evaluation of vortex cores in cerebral aneurysms on 4D flow MR imaging. More sophisticated algorithms are needed to quantify the vortex cores of these aneurysms. Due to the limited spatial and temporal resolution of our 1.5T MR imaging scanner, we may have overlooked small vortex cores that present in a very short time; high-resolution imaging techniques may solve this problem. In addition, the lower signal-to-noise ratio of our MR imaging scanner may have affected the stability of vortex cores; a 3T MR imaging scanner with a head array coil for increasing the signal-to-noise ratio may reduce this effect. In this study, the velocity-encoding value for phase-contrast MR imaging was 40–60 cm/s; it may have compromised our ability to visualize streamlines with minimum velocities on our scans. Studies are underway to identify the optimal velocity-encoding value for the assessment of vortex cores and for determining the aneurysm rupture risk. Our study included only 3 ruptured aneurysms. Large-scale studies may facilitate validation of the role of 4D flow

MR imaging for the assessment of the rupture risk of unruptured cerebral aneurysms. Information on ruptured aneurysms subjected to 4D flow MR imaging studies during the observation period must be collected to determine the role of the complexity and instability of vortex cores in the rupture risk. Because such studies are not prone to the effect of morphologic changes on aneurysm rupture,[16] hemodynamic studies on 4D flow MR imaging may yield the required information.

CONCLUSIONS

Vortex cores in cerebral aneurysms can be identified and evaluated on 4D flow MR imaging. Significantly more aneurysms with-than-without blebs or daughter sacs had a complex flow pattern. Vortex cores of ruptured aneurysms may not be visualized on 4D flow MR imaging. The evaluation of vortex cores on 4D flow MR imaging may help stratify the rupture risk of unruptured cerebral aneurysms.

REFERENCES

1. Cebral JR, Mut F, Weir J, et al. **Association of hemodynamic characteristics and cerebral aneurysm rupture.** *AJNR Am J Neuroradiol* 2011;32:264–70 CrossRef Medline
2. Xiang J, Natarajan SK, Tremmel M, et al. **Hemodynamic-morphologic discriminants for intracranial aneurysm rupture.** *Stroke* 2011;42:144–52 CrossRef Medline
3. Byrne G, Mut F, Cebral J. **Quantifying the large-scale hemodynamics of intracranial aneurysms.** *AJNR Am J Neuroradiol* 2014;35:333–38 CrossRef Medline
4. Jing L, Fan J, Wang Y, et al. **Morphologic and hemodynamic analysis in the patients with multiple intracranial aneurysms: ruptured versus unruptured.** *PLoS ONE* 2015;10:e0132494 CrossRef Medline
5. Jiang M, Machiraju R, Thompson DS, et al. Detection and visualization of vortices. In: Hansen CD, ed. *Visualization Handbook.* Amesterdam: Elsevier Butterworth-Heinemann; 2005:295–309
6. Rütten M, Alrutz T, Wendland H. **A vortex axis and vortex core border grid adaptation algorithm.** *Int J Numer Methods Fluids* 2008;58:1299–326 CrossRef
7. Le TB, Troolin DR, Amatya D, et al. **Vortex phenomena in sidewall aneurysm hemodynamics: experiment and numerical simulation.** *Ann Biomed Eng* 2013;41:2157–70 CrossRef Medline
8. Oeltze-Jafra S, Cebral JR, Janiga G, et al. **Cluster analysis of vortical flow in simulations of cerebral aneurysm hemodynamics.** *IEEE Trans Vis Comput Graph* 2016;22:757–66 CrossRef Medline
9. Meckel S, Stalder AF, Santini F, et al. **In vivo visualization and analysis of 3-D hemodynamics in cerebral aneurysms with flow sensitized 4-D MR imaging at 3 T.** *Neuroradiology* 2008;50:473–84 CrossRef Medline
10. Boussel L, Rayz V, Martin A, et al. **Phase-contrast magnetic resonance imaging measurements in intracranial aneurysms in vivo of flow patterns, velocity fields, and wall shear stress: comparisons with computational fluid dynamics.** *Magn Reson Med* 2009;61:409–17 CrossRef Medline
11. Futami K, Kitabayashi T, Sano H, et al. **Inflow jet patterns of unruptured cerebral aneurysms based on the flow velocity in the parent artery: evaluation using 4D flow MRI.** *AJNR Am J Neuroradiol* 2016;37:1318–23 CrossRef Medline
12. Futami K, Nambu I, Kitabayashi T, et al. **Inflow hemodynamics evaluated by using four-dimensional flow magnetic resonance imaging and size ratio of unruptured cerebral aneurysms.** *Neuroradiology* 2017;59:411–18 CrossRef Medline
13. Lorensen WE, Cline HE. **Marching cubes: a high-resolution 3D surface construction algorithm.** *SIGGRAPH Comput Graph* 1987;21:163–69 CrossRef
14. Shimai H, Yokota H, Nakamura S, et al. **Extraction from biological volume data of a region of interest with nonuniform intensity.** In: *Proceedings of the Society of Photo-Optical Instrumentation Engineers 6051, Optomechatronic Machine Vision.* Kazuhiko Sumi, Japan. December 5–7, 2005; 6051:605115
15. Dormand JR, Prince PJ. **A family of embedded Runge-Kutta formulae.** *J Comput Appl Math* 1980;6:19–26 CrossRef
16. Cornelissen BMW, Schneiders JJ, Potters WV, et al. **Hemodynamic differences in intracranial aneurysms before and after rupture.** *AJNR Am J Neuroradiol* 2015;36:1927–33 CrossRef Medline
17. Cebral JR, Duan X, Chung BJ, et al. **Wall mechanical properties and hemodynamics of unruptured intracranial aneurysms.** *AJNR Am J Neuroradiol* 2015;36:1695–703 CrossRef Medline
18. Köhler B, Gasteiger R, Preim U, et al. **Semi-automatic vortex extraction in 4D PC-MRI cardiac blood flow data using line predicates.** *IEEE Trans Vis Comput Graph* 2013;19:2773–82 CrossRef Medline
19. Marquering HA, van Ooij P, Streekstra GJ, et al. **Multiscale flow patterns within an intracranial aneurysm phantom.** *IEEE Trans Biomed Eng* 2011;58:3447–50 CrossRef Medline
20. Feliciani G, Potters W, van Ooij P, et al. **Multi-scale 3D+t intracranial aneurysmal flow vortex detection.** *IEEE Trans Biomed Eng* 2015;9294:1–8 CrossRef Medline
21. Morita A, Kirino T, Hashi K; UCAS Japan Investigators. **The natural course of unruptured cerebral aneurysms in a Japanese cohort.** *N Engl J Med* 2012;366:2474–82 CrossRef Medline
22. Murayama Y, Takao H, Ishibashi T, et al. **Risk analysis of unruptured intracranial aneurysms: prospective 10-year cohort study.** *Stroke* 2016;47:365–71 CrossRef Medline
23. Tsukahara T, Murakami N, Sakurai Y, et al. **Treatment of unruptured cerebral aneurysms: multi-center study at Japanese national hospital.** *Acta Neurochir Suppl* 2005;94:77–85 CrossRef Medline